13th International Symposium on Particle Image Velocimetry – ISPIV 2019
Munich, Germany, July 22-24, 2019

Development of a High-Speed Plenoptic Imaging System for Time-Resolved 3D-PIV and 3D-PTV

Zu Puayen Tan[1]*, Brian S. Thurow[1]†

[1]Auburn University, Aerospace Engineering, Auburn, USA

*zzt0012@auburn.edu

†thurow@auburn.edu

Abstract

Plenoptic particle image velocimetry (PPIV) has been demonstrated in past literatures as a viable single-/dual-camera technique for 3D flow measurements. Compared to established four-camera tomographic-PIV and 3D-PTV, PPIV has the advantages of lower cost, simpler setup with smaller footprint, a deeper depth-of-field for a given aperture and potential for access to otherwise optically-restricted facilities. However, because camera bodies have to be significantly modified to accommodate an embedded plenoptic microlens array (MLA), past PPIV implementations have been limited to <5*Hz* low-speed Imperx cameras. The mitigation of this short-coming through the development of a modular plenoptic adaptor is hereby presented. The developed adaptor, which consists of an externally-mounted MLA and a pair of relay lenses, attaches to and enables plenoptic capability in unmodified off-the-shelf cameras and intensifiers (including *kHz*-rate high-speed cameras and full-frame sensors), with imaging performance that are comparable to embedded-MLA designs. Results from the use of this adaptor to characterize time-resolved 3D flows around a ctenophore ("sea jelly") is presented, along with preliminary data from the benchmark of the new system's accuracy against a traditional four-camera setup.

1 Introduction

Many flow-fields of industrial and scientific interests exhibit highly unsteady three-dimensional structures. Consequently, 4D flow velocimetry techniques such as tomographic particle image velocimetry (tomo-PIV) and 3D particle tracking velocimetry (3D-PTV) have become the established standards in modern experimental fluid dynamics. Details on these techniques are described by Elsinga et al. (2006), Scarano (2013), Coriton et al. (2014) and Schanz et al. (2016). In spite of tomo-PIV/3D-PTV's effectiveness, these techniques are generally complex to set up and expensive due to the need for four or more imaging cameras. In the effort to reduce equipment cost, simplify installation and enable measurements in optically restricted facilities, a new wave of research is now focused on developing single- or dual-camera alternatives for 4D flow velocimetry. Proposed alternatives include but are not limited to holography (Meng et al., 2004), scanning-mirror 3D-PIV (Bruckers et al., 2013), structured-light illumination (Aguirre-Pablo et al., 2019) and fiber-optics-based or mirror-based view-splitting tomography (see Halls et al., 2018, and Meyer et al., 2016).

As part of this growing trend our group, the Advanced Flow Diagnostics Laboratory (AFDL) at Auburn University, has developed the technique of plenoptic-PIV (PPIV). As described in details by

Lynch (2011), Fahringer & Thurow (2012), Fahringer et al. (2015), and Johnson et al. (2016), PPIV replaces the use of four or more cameras in flow tomography with a single or dual light-field-capturing plenoptic cameras. Shown in Figure 1, the plenoptic imaging process differs from traditional cameras in the addition of a dense microlens array (MLA) in front of the sensor. Through this MLA, light-rays captured by the plenoptic camera's main lens are refocused into a grid of small finite circles on the sensor (instead of a grid of pixel-points in traditional cameras). Each circular sub-image is formed by a single microlens, and pixels within each sub-image encompass rays originating from the same spatial (*s,t*) but different angular (*u,v*) origins. Hence, both spatial and angular information (i.e., the 4D light-field) are preserved in a plenoptic image. Sampling from the grid of sub-images allow the rays' *u,v* and *s,t* information to be recovered, which allows 3D locations of an imaged source to be inferred. Through this method, tomographic 3D reconstruction of a particle field can be performed from as few as a single plenoptic image, followed by 3D cross-correlation for velocimetry.

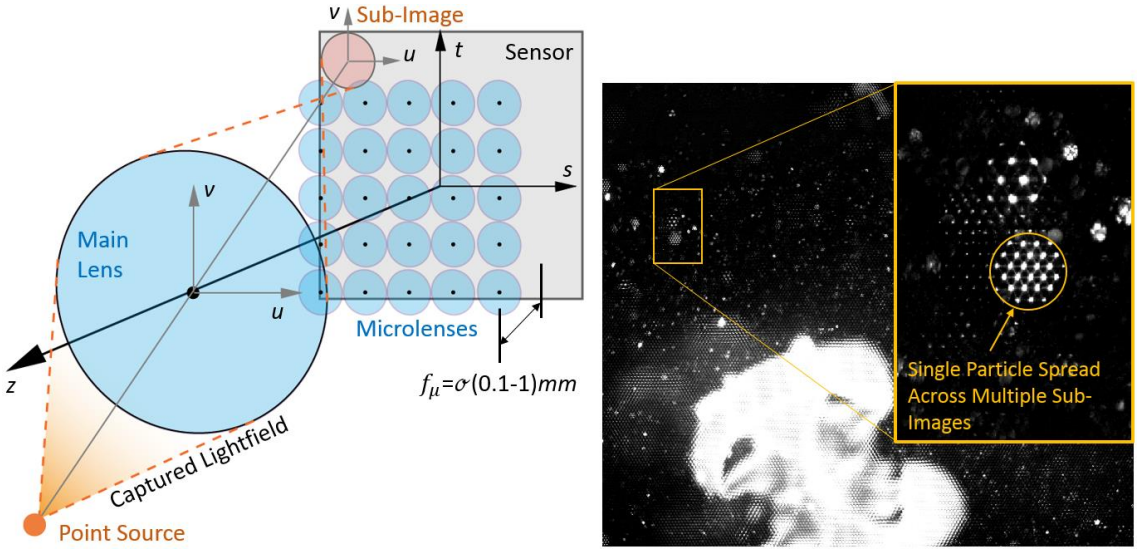

Figure 1. *Left:* Optical configuration of a plenoptic camera. *Right:* A raw plenoptic PIV image.

While the cited past works demonstrated the viability of PPIV, its applications had so far been limited to the use of highly customized Imperx 16 and 29*MP* cameras with embedded on-sensor MLA (see left of Figure 2). Although compact, the embedded-MLA design suffers from several disadvantages:

i. Installation of the MLA requires risky removal of the Imperx camera's sensor-protection glass to locate the MLA within one focal-length (0.1-1*mm*) of the sensor (a requirement for the "Plenoptic 1.0" camera architecture, as described by Georgiev & Lumsdaine (2009)).
ii. The risk of sensor damage during MLA installation so far precludes the use of more expensive high-speed cameras. Thus, PPIV have been limited to <5*Hz* acquisition.
iii. The embedded-MLA design is incompatible with intensified imaging, as intensifiers must be installed between the MLA and camera sensor to spatially encode ray angle information before they are diffused within the intensifier.

To address these disadvantages and enable time-resolved, high-speed PPIV/PTV, AFDL embarked on the development of a modular (off-sensor MLA) plenoptic architecture in 2018. Tan et al. (2019a, 2019b) describes successful benchtop tests of a prototype adaptor, which can be

attached to unmodified off-the-shelf high-speed cameras and intensifiers to enable plenoptic imaging. The matured design of this prototype (dubbed "*DragonEye*") is shown here on the right of Figure 2. Descriptions of *DragonEye* is presented in this paper, along with selected results from field-tests of the device to characterize time-resolved 3D flows around a ctenophore ("sea jelly" creature). Preliminary results are also presented for the validation tests of *DragonEye* against conventional 4-camera tomo-PIV.

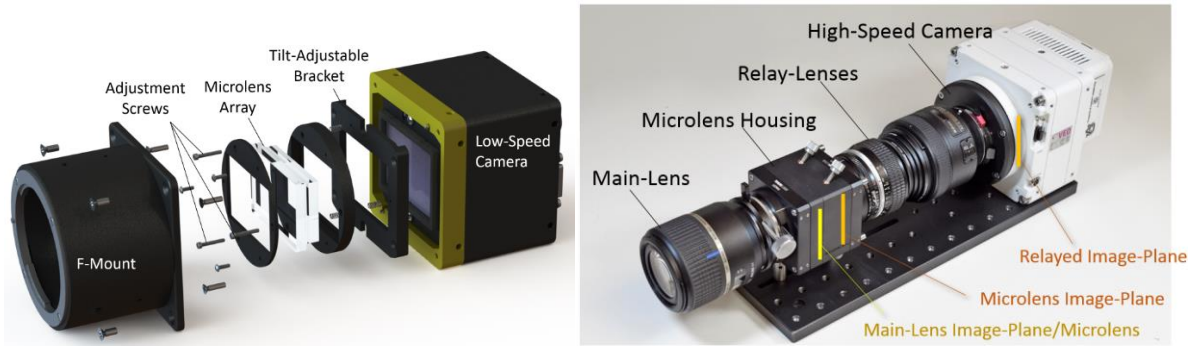

Figure 2. *Left*: An embedded-MLA low-speed plenoptic camera developed at *AFDL* in 2011. *Right*: *DragonEye* installed on Vision Research's Phantom VEO4k 9MP 1kHz high-speed camera.

2 Description of the *DragonEye* Plenoptic Adaptor

Shown on the right of Figure 2, *DragonEye* consists of a cubical chassis that houses an identical full-frame (35*mm*) MLA found in the embedded-MLA cameras. The MLA is floated on springs within the chassis and precisely aligned against the camera's optical axis using three micrometer adjustor screws. Similar to classical embedded-MLA designs, the imaging main-lens that defines the system's magnification and parallax baseline is mounted forwardmost on the assembly. However, unlike past designs, an additional pair of relay-lenses are used on *DragonEye* to project the MLA image-plane downstream into an attached high-speed camera. This projection eliminated the requirement for physically locating the MLA within one focal length of the sensor, thus also eliminating the need to modify existing cameras to accommodate a 36*mm* MLA. Although primarily optimized for Vision Research's VEO4k and VEO640 1*kHz* high-speed cameras, *DragonEye* is largely camera-agnostic and interfaces with any off-the-shelf camera or intensifier through a standard lens mount.

Notably, unlike early prototypes described in Tan et al. (2019a, 2019b) that used a Tamron 60*mm* f/2 macro-lens for 1:1 relay, the current model uses a reverse-mounted Nikon 50*mm* f/1.2 lens focused at infinity to collect and collimate rays from the MLA, followed by either a Nikon 85*mm* f/1.8 or Pentax 70*mm* f/2.4 (also focused at infinity) to focus the rays onto the sensor. Switching to the use of a reverse-mounted collimating lens shortens the minimum MLA-to-relay distance from 100 to 46.5*mm*. This increased the ray-collection angle of the relay lens and significantly reduced the vignette problem encountered in Tan et al. (2019b). The use of a 70-85*mm* second relay lens produces a 1.4-1.7 magnification across the relay system, respectively, which further reduces vignette to a negligible extent, at the expense of some light loss and increased effective system magnification. This unique vignette-mitigation strategy is required because the *DragonEye*/Vision Research combination uses a larger sensor and MLA than most existing relayed-plenoptic designs (see Tan et al. 2019b) to maximize light-collection and image solutions- both critical in PPIV. The large MLA, coupled with the acute angles of light-rays exiting a microlens (compared to a diffused source) made the relay design particularly challenging.

In the current implementation shown in Figure 2, *DragonEye* is matched to a Vision Research Phantom VEO4k camera. Four sets of relay lens and MLA combinations can be used, providing situation-specific optimal performance as outlined in Table 1. Notably, the *M*=1.4 relay configuration provides higher final image resolutions and superior *z*-axis precisions on all MLA designs, while the 70*mm* Pentax lens involved is also a compact pancake lens design. The *M*=1.4 configuration is thus both optically and mechanically preferred. However, the Pentax 70*mm* employs an uncommon K-mount that is not compatible with most high-speed cameras. Hence, the Nikon 85*mm* lens in the *M*=1.7 configuration maximizes camera compatibility at the expense of some optical and mechanical performance. As the 2nd-3rd column of Table 1 shows, employing the existing Imperx camera's hexagonal MLA on *DragonEye* is tenable but results in significantly lower image resolutions. At the same time, the extended DOF (i.e., maximum measurable depth of a plenoptic camera as derived in Fahringer & Thurow, 2018a) is also excessively large relative to the lateral FOV for most applications, while the *z*-axis precision is low. This large DOF characteristic becomes more desirable when the system is used at high magnifications, or when two *DragonEye* are used in a stereo configuration to mitigate *z*-precision issues (as described in Fahringer & Thurow, 2018b).

To balance the system's performance, a new "Small Hexagonal" MLA design was designed for the *DragonEye*-VEO4k combination. The new MLA has significantly smaller pitch and lower F-number, resulting in coarser *u,v* discretization and higher image resolution. The system's extended DOF and *z*-axis precision on the Small Hexagonal MLA are, consequently, more closely matched to that of the existing Imperx 29MP system, while light loss in the 1:1.4-1.7 relay was also partially mitigated due to the lower F-number. Due to availability, results presented in this paper were acquired using only 2011's Hexagonal MLA.

Camera	**Imperx 29MP**	**Vision Research Phantom VEO4k**			
Microlens Type	Hexagonal, 100% fill (2011)			Small Hexagonal, 100% fill (2019)	
Sensor Size (*mm*)	36×24	27.6×15.5			
Sensor Resolution (*px*)	6600×4400	4096×2304			
Full-res frame rate (*fps*)	5	938			
Relay Magnification	-	-1.4	-1.7	-1.4	-1.7
Microlens Pitch (*μm*)	77			36	
Microlens F-number	4			3	
Pixel per Microlens	14	16	19	7.4	9
Final Img Resolution (*px*)	467×311	256×144	211×119	552×311	455×256
Extended DOF (*mm*) at 72*mm* FOV	34.7	139.4	170.7	20.2	25.9
Focal-plane *z*-uncertainty (*mm*) at 72*mm* FOV	4.9	16.5	20.1	5.7	7.0

Table 1. Configurations and performance characteristics of *DragonEye*.

3 Preliminary Results: Ctenophore Swimming Dynamics

Initial field-tests of the *DragonEye* was conducted on the study of unsteady 3D flows around a *Mnemiopsis* ctenophore, performed in collaboration with Auburn University's *Moss Biological Sciences Lab*. An experimental setup consisting of a holding tank with static salt water containing the

ctenophore was used (see Figure 3). A 500mW continuous-wave 532nm laser illuminated the volume, which was filled with 10μm hollow glass spheres for flow seeding. Sufficient time was allowed between the transfer of ctenophore and PPIV acquisition for large bubbles within the water to dissipate. Due to the continuous-wave laser's low intensity and relatively large volume (i.e., low SNR), two *DragonEye*-installed VEO4k cameras were installed, both in forward-scattering, for simultaneous stereo-imaging. Main lens magnifications on cameras 1 and 2 were -0.249 and -0.279, respectively, while relay lens magnifications were -1.7 and -1.4, resulting in a common interrogation volume of 70.6×39.6×34.0mm^3. Volume reconstruction was performed via MART algorithm at a resolution of 7.2vx/mm (or 1.5vx for every microlens in order to adequately sample the hexagonal MLA). Laser light was limited to ~30mm along the center of the tank to minimize reflection artifacts from the tank walls. Due to the low speed of the ctenophore, camera frame-rate was limited to 7.5-15Hz. Standard multi-pass cross-correlation with 50% overlap was used to calculate the velocity-field.

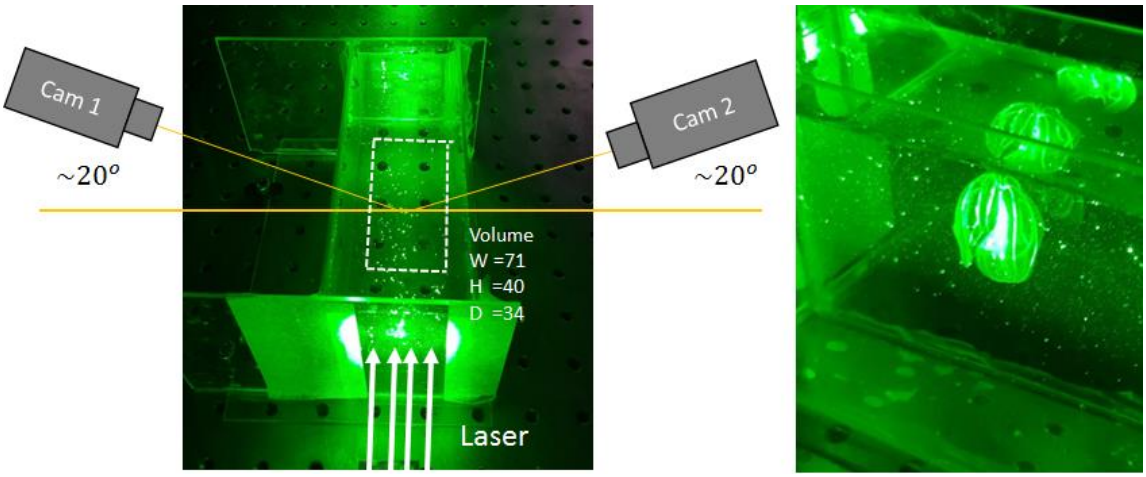

Figure 3. *Left:* experimental setup for characterizing flow-field around a ctenophore. *Right:* example of a ctenophore within the interrogation volume.

Figures 4-7 exhibits preliminary results from the ctenophore study to highlight *DragonEye*'s time-resolved PPIV capabilities. Figure 4 shows the ctenophore in a near-steady swimming state. A series of frames spanning 0.07-5.00s in time is shown on the left, where each streak image consists of 5 instantaneous plenoptic images overlapped to illustrate the motion of particles. In this scene, the ctenophore attempted to propel itself upwards, evident through the drawing-in and deflection of water downwards around the creature. The water surface, however, confined the creature in one spot. In the initial frames the ctenophore's front lobes were pointed down and in an open, relaxed state, while at ~2.5s the creature contracted and maintained this new posture to the end. The right side of Figure 4 shows time traces of simulated particles injected at 0s from multiple rakes in the reconstructed volume/velocity-field. During the 0-5s interval, particles throughout the volume from as far away as the leftmost edge were drawn towards the ctenophore at rates that appear proportional to proximities with the creature. At approximately 5mm from the ctenophore, the particle streams were rapidly deflected downwards to generate propulsive force. The 3D nature of the flow-field, where maximum deflection occurred directly under the creature, is highlighted in Figure 5's rotating views.

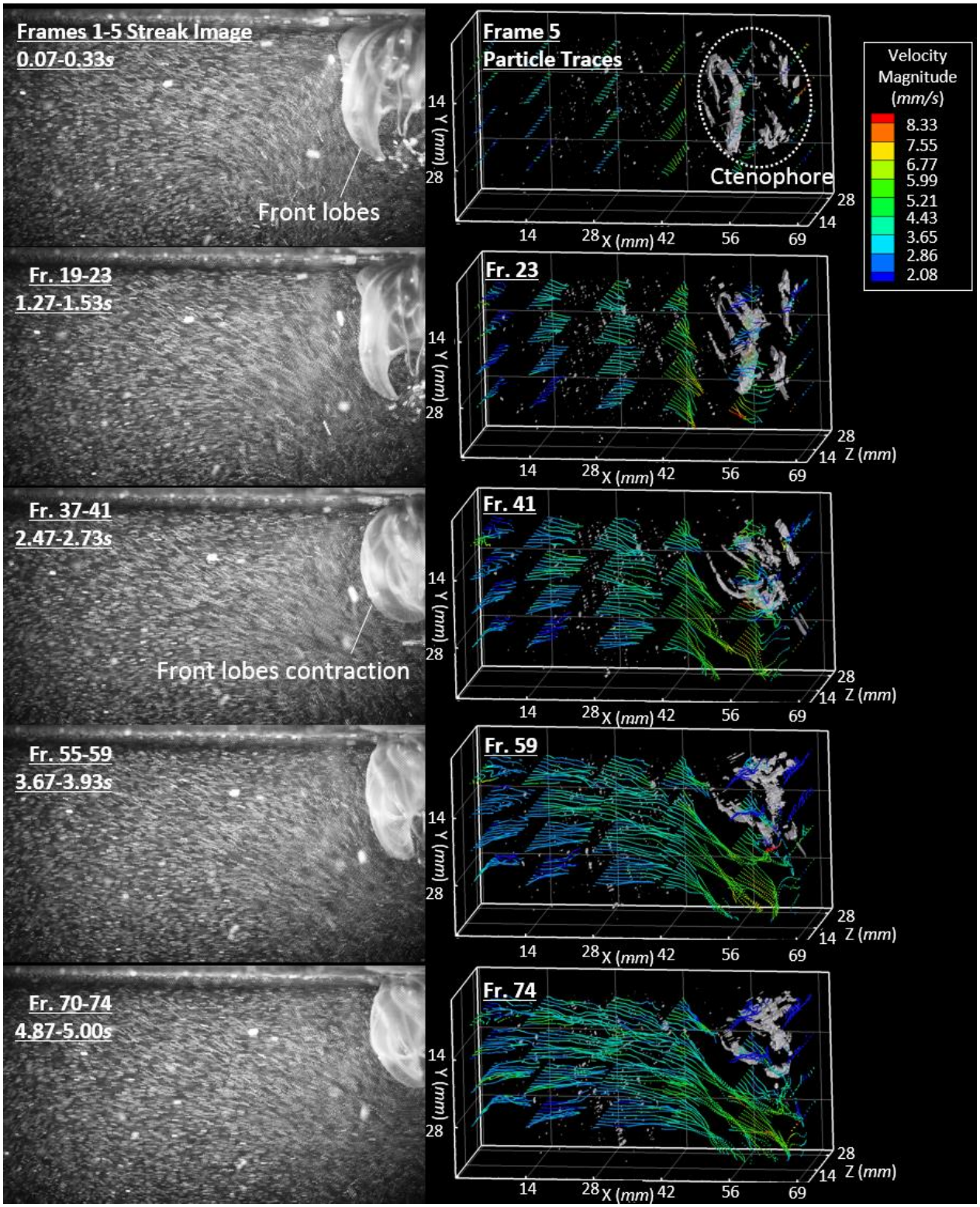

Figure 4. Streak images and 3D particle traces of flow-field around a position-holding ctenophore prior to and after lobe contraction.

Although subtle, streak images in Figure 4 showed that the ctenophor's swimming dynamics changed prior to and after the lobe contraction. This is demonstrated in more detail in Figure 6, which contains two instantaneous central-plane streamlines from the initial and the end of the

sequence. Prior to contraction (Frame 5) the streamlines along the lateral sides of the ctenophore were pointed steeply downwards and have very large velocity magnitudes. I.e., the creature was propelling itself aggressively upwards. Perhaps due to the roundness of the creature, the streamlines can be seen to wrap smoothly around the lower side of the ctenophore. After contraction (Frame 74), not only were flow velocities reduced, the streamlines were oriented generally more horizontally. I.e., propulsion intensity was reduced. It is not clear from the short sequence whether Frame 74 is a weaker swimming state, or whether the ctenophore has ceased swimming and the observed velocities were remaining flow inertia from the prior water movement.

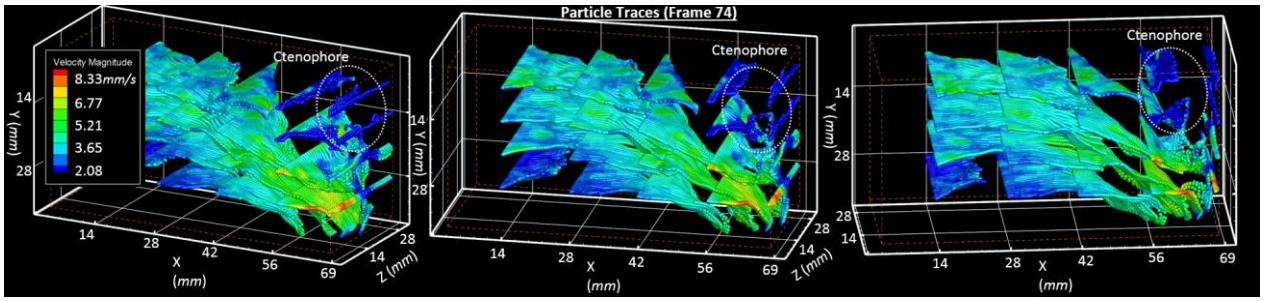

Figure 5. 3D rotation of Frame 74.

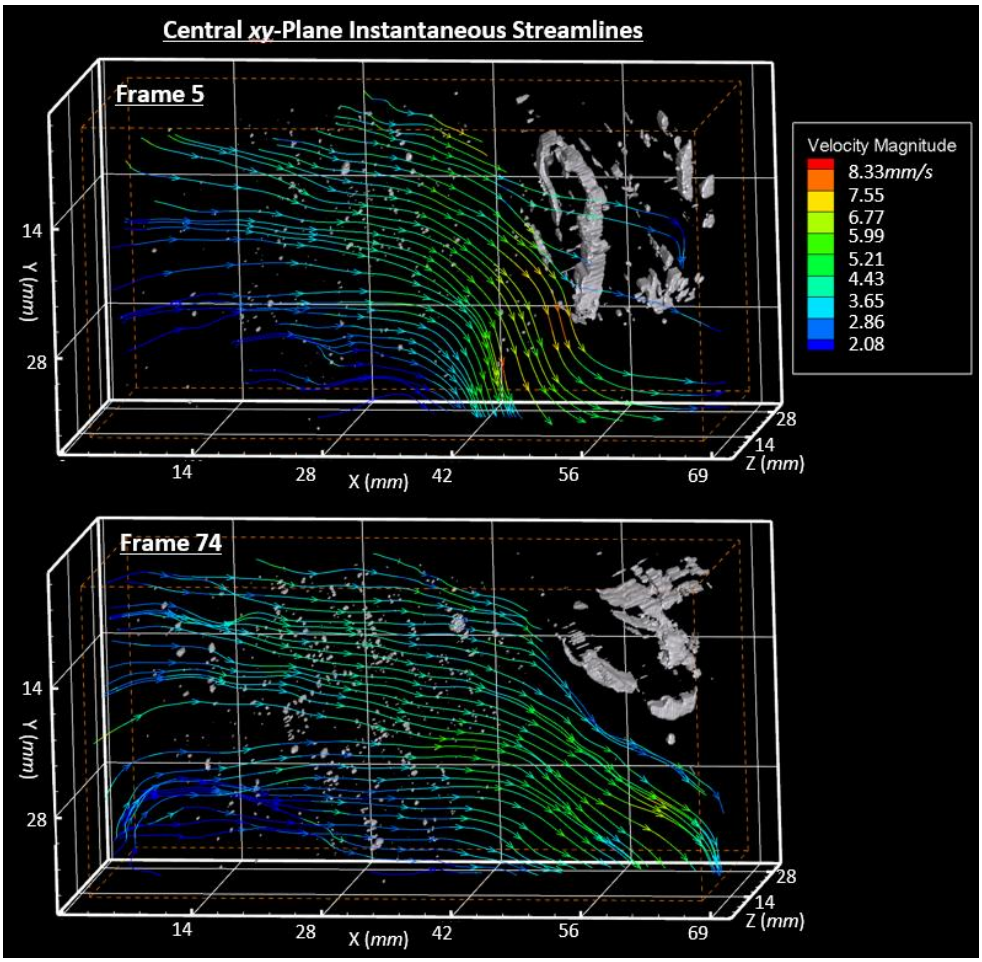

Figure 6. Instantaneous planar streamlines of the position-holding ctenophore before (top) and after (bottom) contraction.

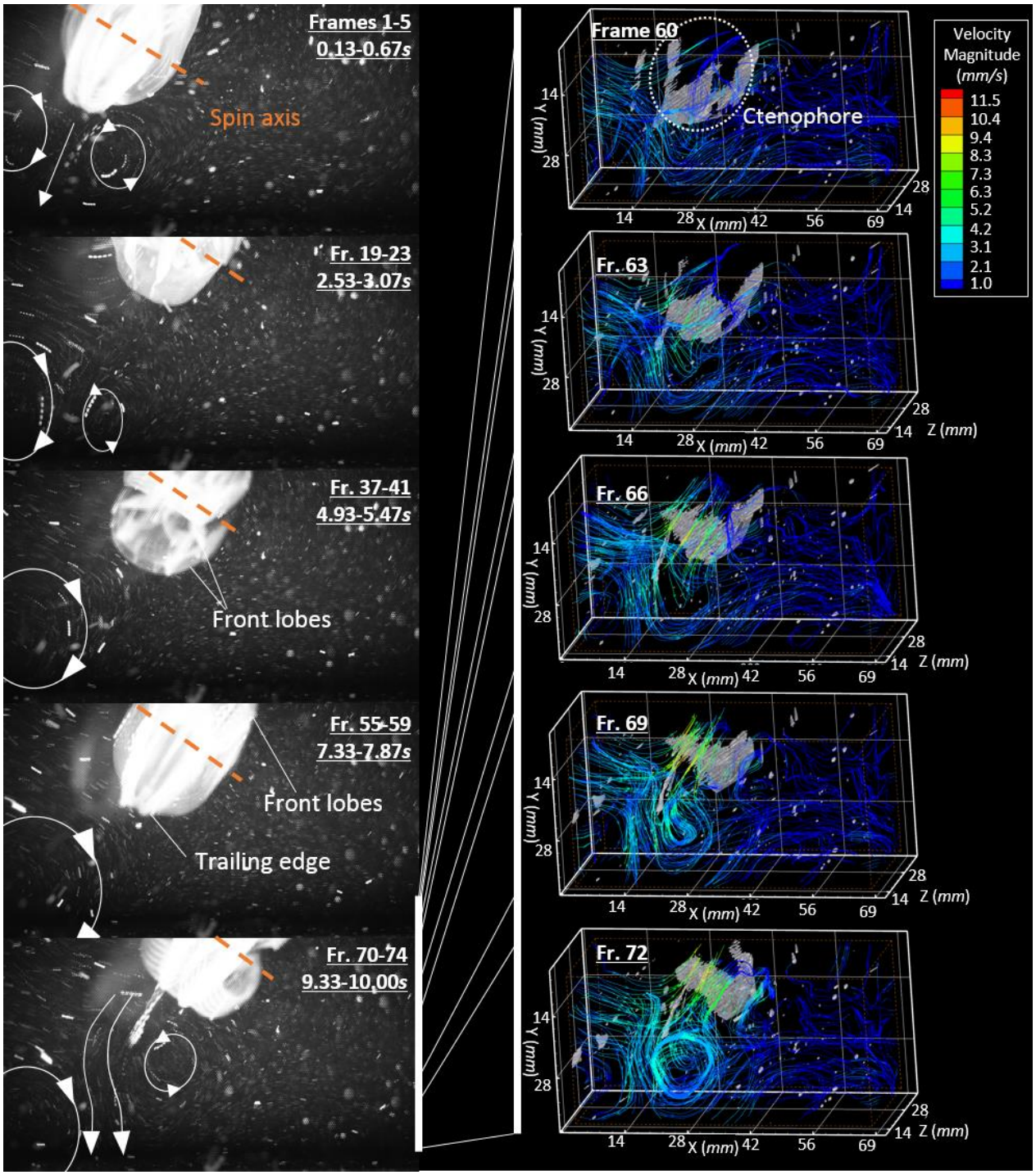

Figure 7. Flow-fields around a spinning and escaping ctenophore, showing the ejection of a vortex ring/tube under rapid acceleration.

While Figures 4-6 showed the ctenophore remaining in a steady position, Figure 7 highlights a more dynamic swimming behavior. On the left, the creature can be seen to spin continuously along an oblique axis in the span of 0.13-10.00*s*, while sporadically ejecting streams of water towards the bottom-left to accelerate towards the top-right. Each acceleration was produced by a jet of water accompanied by vortices that are highlighted by arrows in the streak images. Between Frames 60-75, a large vortex from a previous cycle lingers in the bottom-left as a new smaller vortex was

ejected behind the ctenophore's trailing edge as it accelerated. This process of vortex development was faithfully captured by *DragonEye* and presented as 3D streamlines on the right of Figure 7.

Results presented from Figures 4-7 demonstrated *DragonEye*'s time-resolved PPIV capability, while also representing one of the first detailed characterization of 3D flow-fields around a ctenophore. Analyses are on-going in collaboration with *Moss Biological Sciences Lab* to elucidate the *Mnemiopsis*' swimming dynamics, while developmental efforts are simultaneously devoted to automatic segmentation of the ctenophore from its surrounding particle field in the plenoptic image, in order to separately reconstruct the particle field using MART and the ctenophore (scalar-field) using ART/SART to improve the quality of results.

4 On-Going *DragonEye* Developments

Concurrent with the ctenophore field-tests, efforts were devoted to performance validation of *DragonEye*. The system's volume- and velocity-measurement accuracies were benchmarked against a traditional 4-camera tomo-PIV setup at Purdue University in collaboration with Prof. P. Vlachos' group. Performance of the system using a single (see Figure 8) and dual *DragonEye* in stereo configuration were both tested. In this benchmark test, the cameras were deployed to characterize 3D velocity profiles within a 6.35*mm* diameter tube containing both steady and pulsatile flows, where analytical solutions for the velocity-fields are known. While the camera systems were operated in straddle-frame mode with test-point-dependent *dt*, acquisition rate was maintained at 900*Hz* throughout.

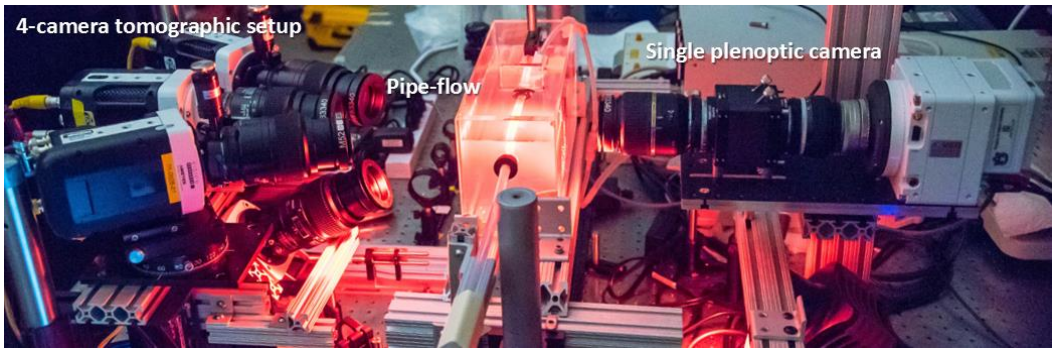

Figure 8. Pipe-flow experimental setup for validation of high-speed plenoptic camera.

To facilitate accurate comparison, volume data from both camera systems were reconstructed using the identical standard MART code suite. The preliminary comparison, as shown in Figure 9, was performed in the domain of 11×10.5×10.5mm^3 centered on the pipe, at a resolution of 45*vx/mm*. Since reconstruction using the traditional tomography setup consisted only of four views while the plenoptic camera contains on the order of 100 views, their solutions are expected to converge in different iteration counts and benefit from different relaxation rates. In this initial result, the 4-camera volume uses 5 iterations and a relaxation of 0.5, while the plenoptic volume uses 4 iterations with no relaxation. Optimization of these parameters remain in progress.

From the initial reconstruction, Figure 9 shows that the same pipe volume can be obtained from both setups. At close inspection in the *xy*-view, particles from both setups can be observed to overlap well. Q-factor analysis to characterize *vx*-to-*vx* correlation between both volumes are expected to be possible once the reconstruction parameters are finalized. The *yz*-views in Figure 9 shows that particles reconstructed from the single plenoptic camera are more elongated

in the *z*-axis compared to the 4-camera setup, because the monocular plenoptic camera suffers from a comparatively narrower parallax baseline. However, the 4-camera volume appears to contain noticeable ghost particles in the regions outside of the pipe border, while the plenoptic volume is relatively ghost-free. Quantification beyond iso-contours is necessary for an exact comparison of ghost particles; however, at first glance the difference is reasonable given that plenoptic cameras benefit from ~100 distinct views per camera, which minimizes the probability of ghosts.

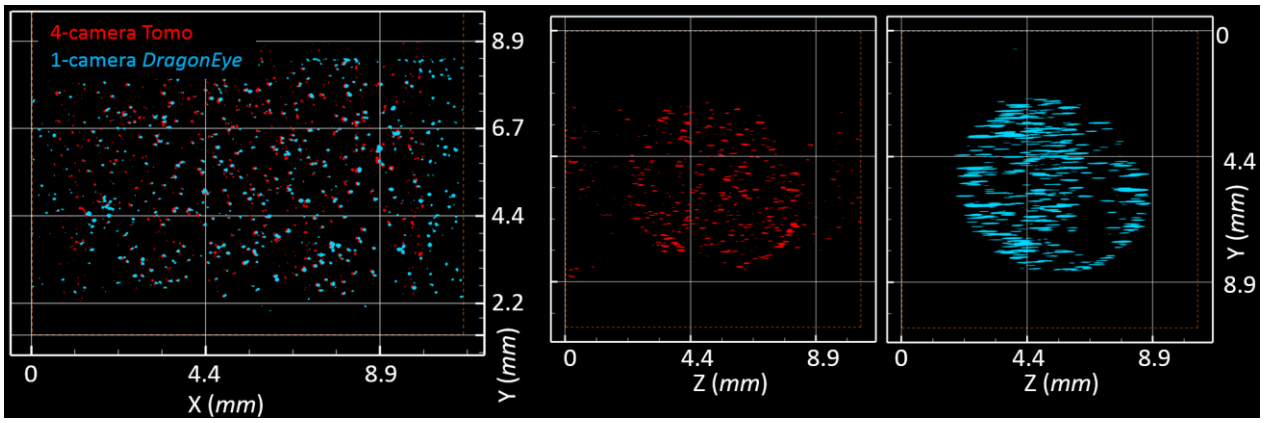

Figure 9. Preliminary comparison between particle fields captured via a 4-camera tomography system and the single-camera *DragonEye* plenoptic system.

Average displacement within the reconstructed volumes in Figure 9 was on the order of 5*vx*. A standard cross-correlation PIV with Gaussian weighting and multi-pass window sizes of [32, 24, 24]*vx* (50% overlap) was performed on the volumes to determine the 3D velocity-fields. Figure 10 compares the calculated velocity-fields for both setups. Velocity distributions along the *yz*-plane (slice-averaged in the *x*-direction) have been plotted on the left, while the right shows single-row velocity distributions across the center of the pipe along the *y* and *z*-directions. Nearly identical velocity profiles were obtained in both cases, with the 4-camera case showing false peaks near the volume's edges in the *z*-direction due to ghost particles. Although the single plenoptic camera has worse precision along the *z*-direction (evident from the *z*-elongation seen in Figure 9), the velocity profile shows no obvious distortion in velocity profile along *z*. A final comparison between the two setups will be performed for different pipe flow velocities once reconstruction parameters are finalized. Additionally, results obtained from two plenoptic cameras in stereo will also be compared.

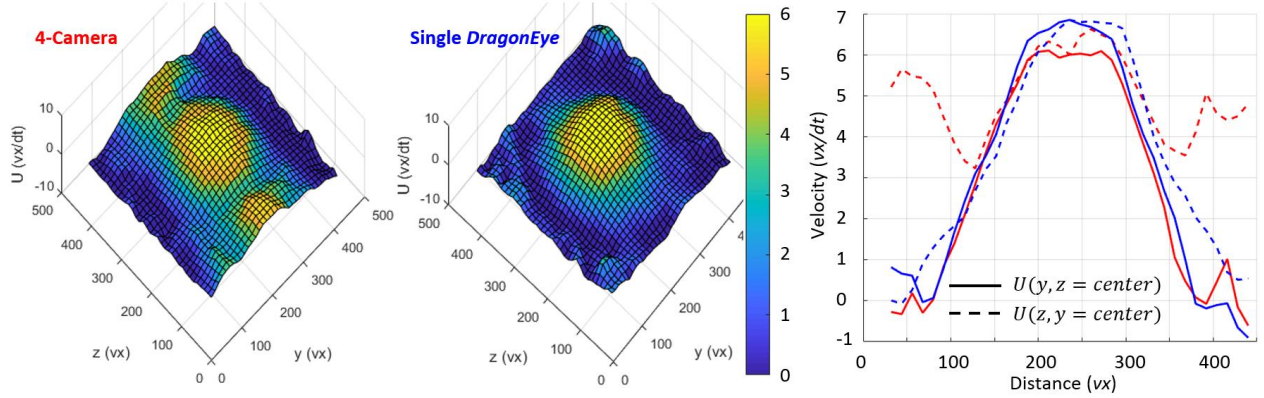

Figure 10. Preliminary comparison of velocity fields.

4 Conclusion and Future Work

Building upon past PPIV works by AFDL, this paper presents a developed modular plenoptic adaptor prototype called the *DragonEye*. In the presented configuration, the *DragonEye* system consists of a front imaging main-lens, a precision-mounted 35*mm* full-frame MLA within an external chassis, followed by a pair of relay-lenses with 1.4-1.7 magnification, and a 1*kHz* Vision Research Phantom VEO4k camera. Two MLA designs were optimized for this configuration, offering an option for large DOF, high-magnification PPIV at 256×144*px* resolution, and a mid-magnification option at 552×311*px* resolution (near-identical to past low-speed PPIV works by AFDL, and higher than other existing relayed-plenoptic designs). Preliminary field-tests of the *DragonEye* to characterize 4D flow-fields around a *Mnemiopsis* ctenophore successfully characterized the animal's steady-state and dynamic swimming modes, including time-resolved recordings of vortex ejections behind the ctenophore as it accelerated within a 70.6×39.6×34.0mm^3 interrogation volume. Benchmark of *DragonEye* against a conventional four-camera tomo-PIV system shows that nearly identical 3D velocity profiles can be obtained for steady flow within a 6.35*mm* diameter pipe. The single camera *DragonEye* system suffers from elongated particles along the *z*-axis due to its limited monocular parallax baseline. However, the elongation was not observed in the preliminary data to affect velocity accuracy, and the availability to ~100 perspective views within the plenoptic camera was observed to produce fewer ghost particles than the four-camera system. Efforts are on-going to optimize MART reconstruction parameters for both camera systems, and more extensive benchmarking comparisons are expected to follow, including volume intensity variance and Q-factor analyses, comparison against analytical velocity profiles, and inclusion of pulsatile flow test-points.

Acknowledgements

Development of the modular, high-speed plenoptic system was carried out under the National Science Foundation's Major Research Instrumentation Program grant No. 1725929. In addition, the authors are also immensely thankful to Prof. Anthony Moss, Richard Alarcon and Johannes Allen at Auburn University for their critical contributions to the ctenophore field-tests; Prof. Pavlos Vlachos, Sayantan Bhattacharya, Javad Eshraghi and Zhongwang Dou's for their involvements in the pipe-flow benchmark experiments at Purdue University; and last but not least, Dr. Eldon Triggs for active support of *DragonEye*'s fabrication at Auburn University.

References

Aguirre-Pablo A A, Aljedaani A B, Xiong J, Idoughi R, Heidrich W, and Thoroddsen S T (2019) Single-camera 3D PTV using particle intensities and structured light. *Experiments in Fluids* 60:25

Brucker C, Hess D, and Kitzhofer J (2013) Single-view volumetric PIV via high-resolution scanning, isotropiv voxel restructuring and 3D least-squares matching (3D-LSM). *Measurement Science and Technology* 24:2

Coriton B, Steinberg A M, and Frank J H (2014) High-speed tomographic PIV and OH PLIF measurements in turbulent reactive flows. *Experiments in Fluids*, Vol. 55:1743

Elsinga G E, Scarano F, Wieneke B, and Oudheusden B W (2006) Tomographic Particle Image Velocimetry. *Experiments in Fluids* 41:6

Fahringer T W and Thurow B S (2018a) The effect of microlens size on the performance of single-camera plenoptic PIV. In *19th International Symposium on the Application of Laser and Imaging Techniques to Fluid Mechanis*, *Lisbon, Portugal*, *July 16-19*

Fahringer T W and Thurow B S (2018b) Plenoptic particle image velocimetry with multiple plenoptic cameras. *Measurement Science and Technology* 29:7

Georgiev T and Lumsdaine A (2009) Superresolution with plenoptic camera 2.0. *Adobe Technical Report*.

Halls B R, Hsu P S, Roy S, Meyer T R, and Gord J R (2018) Two-color volumetric laser-induced fluorescence for 3D OH and temperature fields in turbulent reacting flows. *Optics Letters* 43:12

Lynch K (2011) *Development of a 3-D fluid velocimetry technique based on light field imaging*. Thesis, Auburn University.

Meyer T R, Halls B R, Jiang N, Slipchenko M N, Roy S, and Gord J R (2016) High-speed, three-dimensional tomographic laser-induced incandescence imaging of soot volume fraction in turbulent flames. *Optics Express* 24: 26

Fahringer T W and Thurow B S (2012) Tomographic reconstruction of a 3-D flow field using a plenoptic camera. In *42nd AIAA Fluid Dynamics Conference and Exhibit, New Orleans, Louisiana, USA, June 25-28*

Fahringer T W, Lynch K P, and Thurow B S (2015) Volumetric particle image velocimetry with a single plenoptic camera. *Measurement Science and Technology* 26:11

Johnson K C, Thurow B S, Kim T, Blois G, and Christensen K T (2016) Three dimensional plenoptic PIV measurements of a turbulent boundary layer overlying rough and permeable surfaces. In *18th International Symposium on the Application of Laser and Imaging Techniques to Fluid Mechanics*, *Lisbon, Portugal, July 4-7*

Meng H, Pan G, Pu Y, and Woodward S H (2004) Holographic particle image velocimetry: from film to digital recording. *Measurement Science and Technology* 15:4

Scarano F (2013) Tomographic PIV: principles and practice." *Measurement Science and Technology* 24:1

Schanz D, Gesemann S, and Schroder A (2016) Shake-the-Box: Lagrangian particle tracking at high particle image densities. *Experiment in Fluids* 57:70

Tan Z P and Thurow B S (2019a) Time-resolved 3D flow-measurement with a single plenoptic-camera. In *AIAA SciTech 2019 Forum, San Diego, California, USA, Jan 7-11*

Tan Z P, Johnson K, Clifford C, and Thurow B S (2019b) Development of a modular, high-speed plenoptic camera for 3D flow-measurement. *Optics Express* 27:9